Curr Genet (2014) 60:255–263
DOI 10.1007/s00294-014-0431-4

RESEARCH ARTICLE

A spindle pole antigen gene *MoSPA2* is important for polar cell growth of vegetative hyphae and conidia, but is dispensable for pathogenicity in *Magnaporthe oryzae*

Chao Li · Jun Yang · Wei Zhou · Xiao-Lin Chen · Jin-Guang Huang · Zhi-Hua Cheng · Wen-Sheng Zhao · Yan Zhang · You-Liang Peng

Received: 6 March 2014 / Revised: 24 April 2014 / Accepted: 5 May 2014 / Published online: 25 May 2014

Abstract Spa2 is an important component of the multi-protein complex polarisome, which is involved in the establishment, maintenance, termination of polarized cell growth and is important for defining tip growth of filamentous fungi. In this study, we isolated an insertional mutant of the rice blast fungus *Magnaporthe oryzae* that formed smaller colony and conidia compared with the wild type. In the mutant, a spindle pole antigen gene *MoSPA2* was disrupted by the integration of an exogenous plasmid. Targeted gene deletion and complementation assays demonstrated the gene disruption was responsible for the defects of the insertional mutant. Interestingly, the MoSpa2-GFP fusion protein was found to accumulate as a spot at hyphal tips, septa of hyphae and conidial tip cells where germ tubes are usually produced, but not in appressoria, infection hyphae or at the septa of conidia. Furthermore, the deletion mutants of *MoSPA2* exhibited slower hyphal tip growth, more hyphal branches, and smaller size of conidial tip cells. However, *MoSPA2* is not required for plant infection. These results indicate that *MoSPA2* is required for vegetative hyphal growth and maintaining conidium morphology and that spotted accumulation of MoSpa2 is important for its functions during cell polar growth.

Keywords Polarisome · Polarized growth · Morphogenesis · The rice blast fungus · Vegetative hyphal growth

Introduction

Hyphal tip growth is a key feature of filamentous fungi. To support the tip growth, a specialized apparatus is required, which contains five major components: the Spitzenkorper, the polarisome, the exocyst, recycling endocytosis, and Cdc42 GTPase module (Harris 2009; Jones and Sudbery 2010; Kohli et al. 2008; Lichius et al. 2012). In the budding yeast *Saccharomyces cerevisiae*, the polarisome was identified as a 12S multi-protein complex that is consist of Spa2, Pea2, and Bud6/Aip3, and interacts with Bni1 (Sheu et al. 1998). Besides, it has been observed that Msb3 and Msb4 bind to the N-terminal of Spa2, suggesting that these two proteins are also components of the polarisome (Tcheperegine et al. 2005). Spa2 is a scaffold protein physically interacting with all other polarisome components through specific binding domains (Sheu et al. 1998; van Drogen and Peter 2002). Spa2 is involved in the direction and control of cell division, and localizes to the site of cell growth (Gehrung and Snyder 1990; Roemer et al. 1998). Bud6 is an actin-binding protein, which has an additional function in microtubule plus-end capture at the cell cortex, with contributions of formins (Amberg et al. 1997; Delgehyr et al. 2008). Pea2 was shown to be

Communicated by S. Hohmann.

Nucleotide sequence data are available in the GenBank database under the accession number KF201869 (*MoSPA2*).

Electronic supplementary material The online version of this article (doi:10.1007/s00294-014-0431-4) contains supplementary material, which is available to authorized users.

C. Li · J. Yang · W. Zhou · X.-L. Chen · J.-G. Huang · Z.-H. Cheng · W.-S. Zhao · Y. Zhang · Y.-L. Peng (✉)
Ministry of Agriculture Key Laboratory of Plant Pathology, Department of Plant Pathology, China Agricultural University, Beijing 100193, China
e-mail: pengyl@cau.edu.cn

J. Yang
e-mail: yangj@cau.edu.cn

important for the stability and localization of Spa2 (Valtz and Herskowitz 1996).

SPA2 orthologous genes have been identified in a number of ascomycetous fungi, and this protein family seems to be conserved. In *Ashbya gossypii*, *AgSPA2* is required for area determination of growth at hyphal tip (Knechtle et al. 2003). In *Aspergillus nidulans*, Spa2 homologs localize to hyphal tips, where they regulate hyphal morphology and the rate of hyphal extension (Virag and Harris 2006), and the *Aspergillus niger* SpaA was suggested to play a role in ensuring maximal polar growth rate (Meyer et al. 2008). In *Candida albicans*, *CaSPA2* was found to be important for virulence (Zheng et al. 2003). However, in the basidiomyceteous pathogen *Ustilago maydis, SPA2* was dispensable for pathogenicity (Carbo and Perez-Martin 2008).

In this study, we isolated and functionally characterized an *SPA2* orthologous gene in the rice blast fungus *Magnaporthe oryzae*. Deletion of *MoSPA2* led to slow vegetative hyphal growth and unusual branching of vegetative hyphae. *MoSPA2* is also important to maintain normal size of conidia. In the strain expressing the MoSpa2-GFP fusion, accumulated green fluorescence signals as a spot could be observed at vegetative hyphal tips, septa of hyphae and conidial tip cells where germ tubes are usually produced but not in appressoria, infection hyphae and at the septa of conidia. Furthermore, *MoSPA2* was found to be dispensable for plant infection.

Table 1 Fungal strains used in this study

Strain	Description	References
P131	A wild-type strain	Peng and Shishiyama (1988)
S1528	A wild-type strain	Yang et al. (2010)
X6149	An ATMT mutant	This study
CM20	X6149 expressing the wild-type *MoSPA2*	This study
MH1	A deletion mutant of *MoSPA2*	This study
MH2	A deletion mutant of *MoSPA2*	This study
CG12	MH1 expressing the *MoSPA2-GFP*	This study

Table 2 PCR primers used in this study

Name	Sequence (5′ → 3′)
Upf	CATACTAGTTACGAACAACTCTGGGTCAC
Upr	CATCTGCAGGTTTAGTGCTCGCAAGTGTATG
downf	CATATCGATGGAGTTGTCTGTGTTTGTTCTC
downr	CATGGTACCCGAGTGACACGGGTTAGAT
Out	ACGGTTATGTGTGGGAGATAC
hptup	GACAGACGTCGCGGTGAGTT
Inf	TCACCAAGTTCCAGGTTGC
Inr	TCCTTTGACTCTCTGGCGA
Hbup	GATGGATCCATGAACGCTGCTGCCACC
hbdown	CATTCTAGATGAAAAGTCATCACCACCAC
spa2gfpf	CATGGTACCGTAGCTACCTTAGTAACCTTGG
spa2gfpr	CATTCTAGATGAAAAGTCATCACCACCACCAG

Materials and methods

Strains and growth conditions

The wild-type strain P131 and its various transformants generated in this study (Table 1) were cultured at 25 °C on oatmeal tomato agar (OTA) plates (Peng and Shishiyama 1988; Yang et al. 2010). Mycelia collected from 2-day-old cultures in complete medium shaken at 150 rpm were used for isolation of fungal genomic DNA and protoplasts. Protoplasts were isolated and transformed with the PEG/$CaCl_2$ method (Park et al. 2004). Media were supplemented with 250 μg/ml hygromycin B (Roche, USA) or 400 μg/ml neomycin (Ameresco, USA) to select hygromycin-resistant or neomycin-resistant transformants, respectively. Genetic crosses were performed as described by Talbot et al. (1996).

Nucleic acid manipulation

Genomic DNAs were extracted from vegetative hyphae with the CTAB protocol (Xu and Hamer 1996). Standard protocols of molecular biology were followed for plasmid isolation, DNA gel blot analyses, and DNA enzymatic digestion (Sambrook and Russell 2001). Probes were labeled with the random primer labeling kit (TaKaRa, Dalian, China). Plasmid constructs were sequenced with an ABI 3730 sequencer (SunBio Company, China). Reverse transcription assays were performed with the PrimeScript RT-PCR Kit (TaKaRa, Dalian, China). All primers (Table 2) were synthesized by Sangon (Shanghai, China).

Identification of *MoSPA2*

A restriction enzyme-mediated DNA integration (REMI) mutant X6149 was generated by transforming the plasmid pUCATPH into the wild-type strain P131 (Lu et al. 1994; Yang et al. 2010). Flanking sequences of the insertion site were isolated using the plasmid rescue approach (Sweigard et al. 1998) and was determined with an ABI 3730 sequencer (SunBio Company, China). BLASTn and BLASTp were used to search for DNA and protein sequences in the GenBank nr database. Protein sequence comparisons and alignment analysis were performed with

ClustalX (Saitou and Nei 1987), ESPript (Gouet et al. 1999), and MEGA4 (Tamura et al. 2007).

Complementation assay

The *MoSPA2* complementation vector pCSPA2 was constructed by cloning *MoSPA2* along with its 1.3-kb upstream sequence and 0.5-kb downstream sequence, which was amplified with the primer pair hbf/hbr (Table 2) into pKN (Yang et al. 2010). After linearization with *Dra*I, pCSPA2 was introduced into the mutant X6149. The resulting transformants were confirmed to harbor a single copy of pCSPA2 by DNA gel blot.

Generation of the *MoSPA2* deletion mutants

For generating the *MoSPA2* gene replacement vector pKSPA2, the 1.74-kb upstream and 0.83-kb downstream sequences of *MoSPA2* were amplified with primer pairs upf/upr and downf/downr, respectively. The resulting PCR products were cloned into the *Spe*I–*Pst*I and *Cla*I–*Kpn*I sites of pKNH, respectively (Yang et al. 2010). After linearization with *Not*I, pKSPA2 was transformed into P131. Hygromycin-resistant transformants were isolated and assayed for resistance to neomycin. The transformants were further screened by PCR with the primer pair inf/inr and out/hphup. The putative *Mospa2* null mutants were further confirmed by DNA gel blot.

Generation of the *MoSPA2-eGFP* fusion

The *MoSPA2–eGFP* fusion vector pKGSPA2 was generated by cloning *MoSPA2* along with its 1.2-kb upstream sequence, which was amplified with the primer pair spa2gfpf/spa2gfpr (Table 2) into pKNTG (Yang et al. 2010). After linearization, pKGSPA2 was transformed into the *ΔMospa2* null mutant.

Plant infection

A 4-week-old seedlings of the rice cultivar 'LTH' and 8-day-old seedlings of barley cultivar 'E9' were used for infection assays. For the infection assay, conidial suspensions with a concentration of 5×10^4 conidia/ml were sprayed on to the plant leaves, and the inoculated plants were incubated as previously described (Peng and Shishiyama 1988). Lesions were examined and photographed 5–7 days post-inoculation (dpi).

Microscopy

Conidia were inoculated on to barley epidermis cells, and the infection process was observed at 24 and 48 h post-inoculation (hpi). Nuclei and septa were visualized using Hoechst 33258 (Sigma) at 1 μg/ml and Calcofluor White (Sigma) at 10 μg/ml, respectively (Du et al. 2013; Xu and Hamer 1996). Samples were observed and photographed under a Nikon Ni90 fluorescence microscope (Nikon, Japan).

Results

Isolation of the mutant X6149

To identify genes that are important for asexual development and pathogenesis in *M. oryzae*, we screened the REMI library established in our laboratory (Yang et al. 2010). One mutant, X6149, was isolated after screening over 8,000 transformants and found to be exhibited impaired growth. When incubated on OTA plates for 5 days, the average size of the wild-type colony was 40 mm in diameter, whereas X6149 was only 23 mm (Fig. 1a). To determine whether the defects of X6149 were caused by an REMI event, a genetic cross was made between X6149 (*MAT* 1-1) and a wild-type strain S1528 with the opposite mating type (*MAT* 1-2). Among the 34 progeny isolated, all of the 19 hygromycin-susceptible progeny exhibited the wild-type phenotype, and the remaining 15 hygromycin-resistant progeny showed the same defects in colony growth as X6149. These data

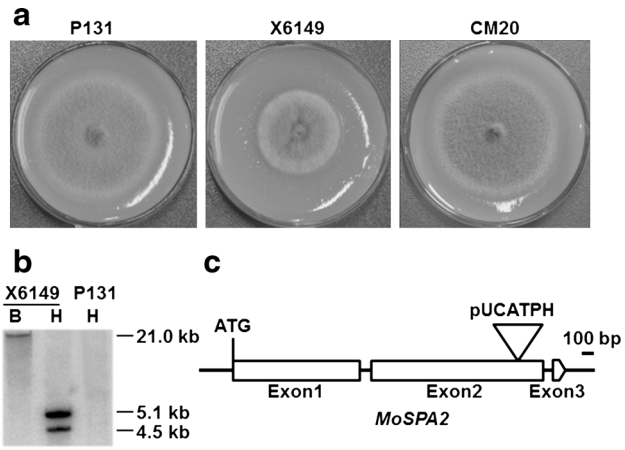

Fig. 1 *MoSPA2* was isolated from an REMI mutant X6149. **a** Colonies of the wild-type P131, the mutant X6149, and one complementation transformant CM20 cultured on OTA plates at 5 dpi. **b** DNA gel blot analysis of genomic DNA of X6149 and P131 digested with *Hin*dIII or *Bgl*II and probed with the hygromycin phosphotransferase (*hph*) gene cassette. The estimated sizes of each band are labeled at *right* (kb). **c** *Schematic diagram* showing the exogenic plasmid pUCATPH integrated into *MoSPA2* (MGG_03703.6). *Rectangles* indicate exons of *MoSPA2*, *ATG* represents the putative translation start site, and the *triangle* indicates the integration site of pUCATPH

indicated that the defect in colony growth of X6149 was co-segregated with the hygromycin gene and there was only a single integration site of the exogenous DNA in the genome of this mutant. DNA gel blot hybridization probed with the transforming vector pUCATPH revealed that the mutant X6149 had one 21.0-kb *Bgl*II hybridizing band and two 5.1- and 4.5-kb *Hin*dIII hybridizing bands (Fig. 1b), indicating that there was only a single integration site of the exogenous DNA in the genome of this mutant, and the exogenous DNA should have two copies.

Identification of *MoSPA2*

From the mutant X6149, a 13.0-kb plasmid pXB13 with 3.0-kb chromosomal DNA flanking the pUCATPH insertion was isolated. Further sequence analyses showed that the insertion occurred at the second exon of an open reading frame, *MGG_03703.6* (Fig. 1c). The deduced protein encoded by this gene shared 50 % identity with Spa2p (GenBank Access No. NP_013079) of *S. cerevisiae*, and hence was named as *MoSPA2*. To confirm that *MoSPA2* was responsible for the defects of X6149, we carried out a complementation assay by introducing the vector pCSPA2 into X6149. Twenty-three complementation transformants were obtained and several of them, including CM20, were confirmed to harbor a single copy of pCSPA2 by DNA gel blot (data not shown). The colony diameter of CM20 (40 mm) was completely restored to the wild-type level (40 mm) at 5 days post-inoculation (dpi) on OTA plates (Fig. 1a). These results indicated that *MoSPA2* was responsible for the defects in vegetative hyphal growth of X6149.

The 3,005-bp open reading frame of *MoSPA2* is interrupted by two introns, whose positions were verified by sequencing of the corresponding cDNA. The deduced 951 amino acid sequence has a predicted molecular mass of 103.96 kDa with a *pI* of 5.21 and shows high degree of overall homology with the Spa2 homologous proteins from other Ascomycetes (Fig. S1). When comparing MoSpa2 with *S. cerevisiae* Spa2, a common domain named SHD-I (Roemer et al. 1998) could be identified. The amino acid sequence of MoSpa2 SHD-I domain exhibited 46 % similarity with other Ascomycetes sequences. Remarkably, the Spa2 direct repeat (SDR, A(R/Q)xKLxxLxxx(R/Q)Fx(D/E)LxxDVxxELxRR; Roemer et al. 1998) located in the SHD-I domain seems to be extremely conserved from yeast to filamentous fungi (Fig. S2), suggesting that the SDR plays crucial role for protein function.

Generation of the deletion mutants of *MoSPA2*

To further define functions of *MoSPA2*, we generated a gene replacement vector pKSPA2 by replacing the *MoSPA2* ORF with a hygromycin phosphotransferase gene cassette (*hph*) (Fig. 2a). Two putative *MoSPA2* deletion mutants, MH1 and MH2, were verified by PCR and confirmed by DNA gel blot (Fig. 2b). The 2.1-kb band amplified with the primer pair out/hphup was detected only in the putative *Mospa2* null mutants, while a 1.2-kb band amplified with primer pair inf/inr was detected only in the wild-type P131 (data not shown). When probed with a 0.83-kb fragment amplified from pKSPA2 with primer pair downf/downr, the putative *MoSPA2* deletion mutant had one hybridizing 6.5-kb *Hin*dIII fragment instead of the hybridizing 2.0-kb fragment of the wild-type P131. The *MoSPA2* transcript was also detected by RT-PCR in the wild-type P131 and complementation strain CM20, but not in the knockout mutants (Fig. 2c).

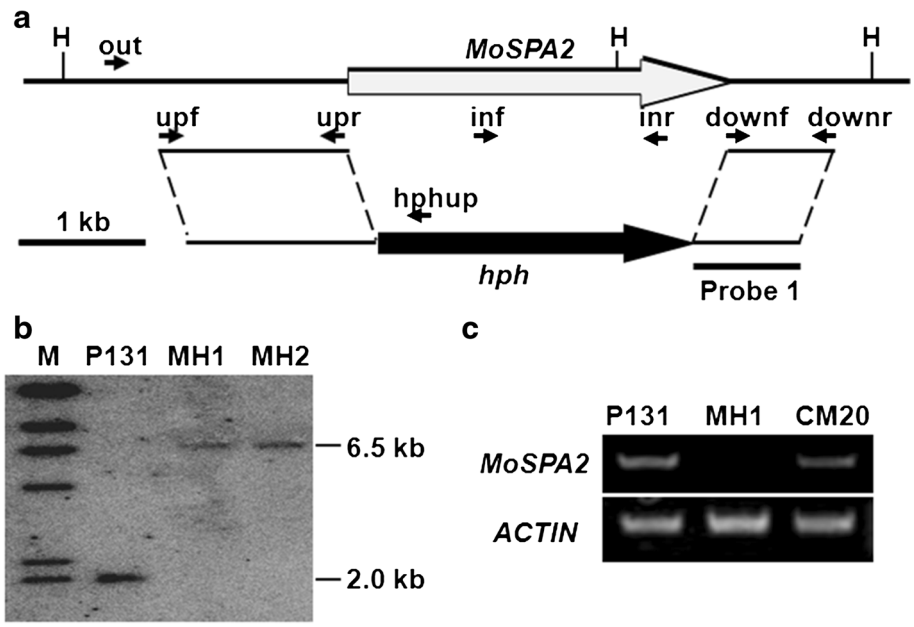

Fig. 2 The *MoSPA2* knockout vector and gene replacement mutants. **a** The *MoSPA2* knockout vector was constructed by amplifying the upstream and downstream flanking sequences with primer pair upf/upr and downf/downr, respectively, and ligated with the *hph* cassette. H, *Hin*dIII. **b** DNA gel blot analysis of *Hin*dIII-digested genomic DNAs of the wild-type P131 and two *ΔMospa2* null mutants MH1 and MH2 hybridized with Probe 1. The estimated size of each band is labeled at *right* (kb). **c** RT-PCR was used to confirm the loss of *MoSPA2* transcripts from the *ΔMospa2* null mutant MH1. Actin was used as a control

Deletion of *MoSPA2* affects hyphal growth and branching

To determine the role of *MoSPA2* on vegetative hyphal growth, the *ΔMospa2* null mutant, the wild-type P131, and one complementation transformant CM20 were incubated on to OTA plates for 5 days. While the wild-type strain and the complementation transformant formed a fluffy and grayish colony, the *ΔMospa2* null mutant formed a smaller darker colony (Fig. 3a). The average diameter of the wild type and the complementation transformant colonies was approximately 40 mm at 5 dpi. Under the same conditions, the diameter of the *ΔMospa2* colonies was only 27 mm (Fig. 3b). When stained with Calcofluor White, the vegetative hyphae of the *ΔMospa2* null mutant exhibited significantly more septa than those of the wild type and the complementation transformant (Fig. 3c). The average length of sub-apical hyphal cells in the *ΔMospa2* null mutants was 49.4 μm, which was significantly shorter than the 84.5 μm of the wild type and the 84.6 μm of the complementation transformant (Fig. 3d). In addition, the average length of secondary apical hyphal cells in the *ΔMospa2* null mutants was 51.3 μm, which was also significantly shorter than the 85.4 μm of the wild type and the 83.9 μm of the complementation transformant (Fig. 3d). When co-stained with Hoechst 33258 and Calcofluor White, one nucleus was detected in each cell compartment of the

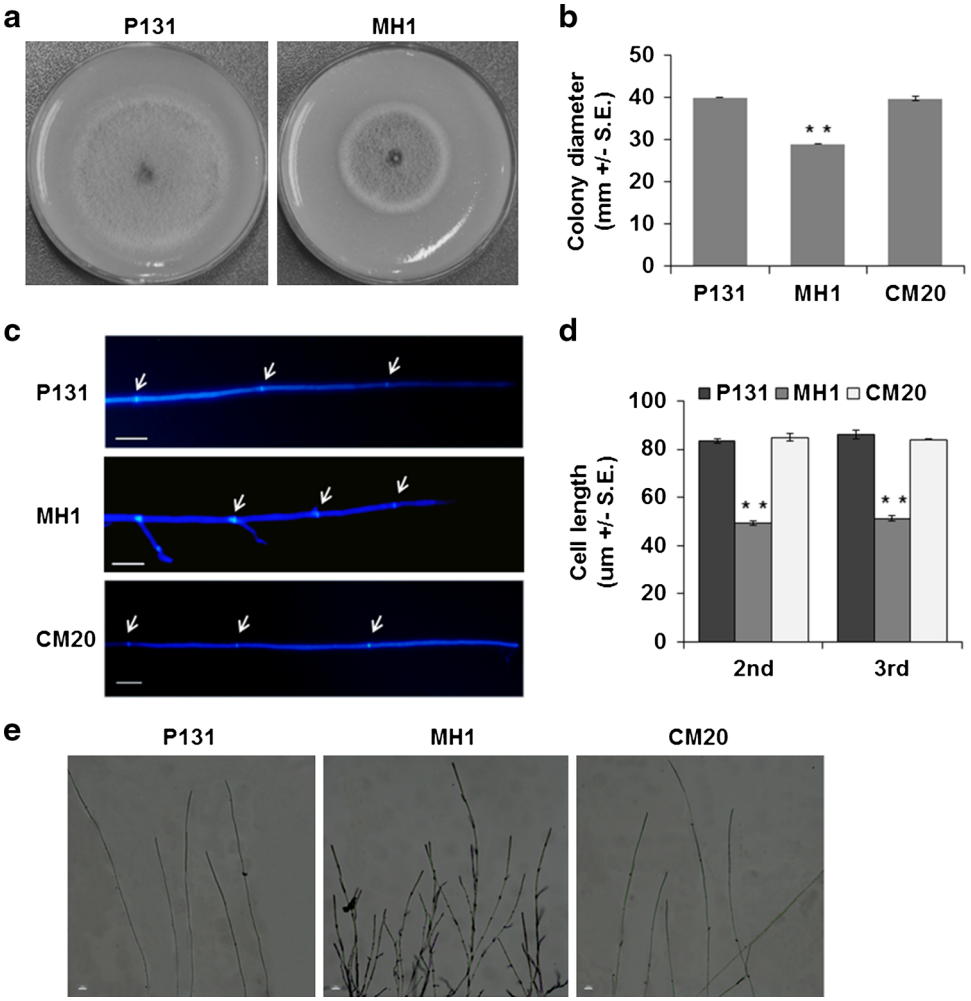

Fig. 3 *MoSPA2* is required for vegetative hyphal growth. **a** Colony of the wild-type P131 and the *ΔMospa2* null mutant MH1 cultured on OTA plates at 5 dpi. **b** The colony diameter of the strains at 5 dpi. The data represent the mean values of a quadruple experiment with a standard deviation. *Asterisks* indicate a significant difference in the colony diameter between the *ΔMospa2* null mutant and the wild-type strain (or complementation strains) at $p = 0.01$ according to t test. **c** Vegetative hyphae of P131, MH1, and CM20 stained with Calcofluor White. *White arrows point* to the septa. *Bar* 20 μm. **d** The average length of the sub-apical cells and secondary-apical hyphal cells of vegetative hyphae in P131, MH1, and CM20. Means and standard deviations were calculated based on three independent experiments by measuring at least 50 mycelia in each replicate. *Asterisks* indicate a significant difference in the cell length between the *ΔMospa2* null mutant and the wild-type strain (or complementation strains) at $p = 0.01$ according to t test. **e** The branch pattern of vegetative hyphae in P131, MH1, and CM20 on cover glass at 2 dpi. *Bar* 10 μm

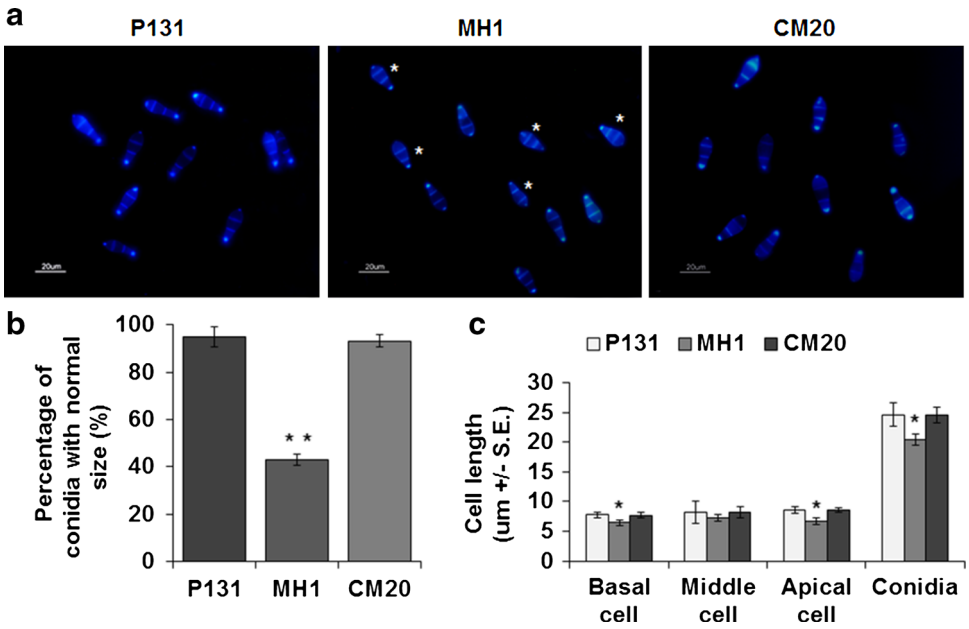

Fig. 4 *MoSPA2* is required for maintaining conidium morphology. **a** Conidia of the wild-type P131, the *ΔMospa2* null mutant MH1, and one complementation strain CM20 stained with Calcofluor White. *White asterisks* in central panel point to abnormal conidia. *Bar* 20 μm. **b** The percentage of conidia with normal size in P131, MH1, and CM20. *Asterisks* indicate a significant difference between the percentage of conidia with normal size of the mutant and wild-type strain (or complementation strain) at $p = 0.01$ according to *t* test. **c** Average length of the basal, middle, and apical cell of the conidia by P131, MH1, and CM20 and the total length of the conidia. Means and standard deviations were calculated based on three independent experiments by measuring at least 100 conidia in each replicate. *Asterisks* indicate a significant difference of the cell length of conidia between the mutant and the wild-type strain (or complementation strain) at $p = 0.05$ according to *t* test

vegetative hyphae of the wild-type strain, the complementation transformant and the *ΔMospa2* null mutant (Fig. S3). The *ΔMospa2* null mutant also displayed a lower radial colony growth rate and produced more apical and sub-apical branches than the wild-type P131 and the complementation transformant CM20 (Fig. 3e). These results indicate that *MoSPA2* plays a role in polarity maintenance and is required for maximal polar growth rate.

MoSPA2 is important for conidium morphology

We stained the conidia with Calcofluor White to observe whether disruption of *MoSPA2* had any effects on conidium morphology. The *ΔMospa2* null mutant was found to produce smaller conidia (Fig. 4a), and about 60 % of the *ΔMospa2* conidia were smaller than that of the wild type (Fig. 4b). On average, conidia from the wild type and the complementation transformant were 24.5 and 24.6 μm in length, respectively. In contrast, the *ΔMospa2* conidia were approximately 20.4 μm in length (Fig. 4c). In comparison with the wild-type conidia, the lengths of the basal and apical cells of the *ΔMospa2* conidia were significantly reduced than the middle ones (Fig. 4c). Therefore, *MoSPA2* is required for maintaining normal conidium morphology.

The expression pattern of *MoSPA2*

To investigate the expression pattern of *MoSPA2*, a 1.2-kb fragment of the *MoSPA2* promoter was amplified and cloned into the vector pKNTG. The resulting plasmid pKGSPA2 containing the enhanced green fluorescent protein (eGFP) was introduced into the *ΔMospa2* null mutant. One of the resulted transformants, CG12, which carried a single copy insertion of pKGSPA2 and restored the wild-type colony growth and conidial morphology, was selected for analyzing sub-cellular localization and expression pattern of MoSpa2. The green fluorescence signals were easily observed in the cytoplasm of conidia and appressoria (Fig. 5a), but was obscurely observed in infection hyphae. Interestingly, an obvious aggregation of green fluorescence signals was observed at the tip of apical or basal cell of conidium where germ tube was produced (Fig. 5a). We also examined the sub-cellular localization of MoSpa2-GFP in vegetative hyphae. In all of more than 300 vegetative hyphae, a strong aggregation of green fluorescence signals was observed at each hyphal tip (Fig. 5b). Moreover, strong green fluorescence signals were observed at the septum of vegetative hyphae but not of conidia (Fig. 5b).

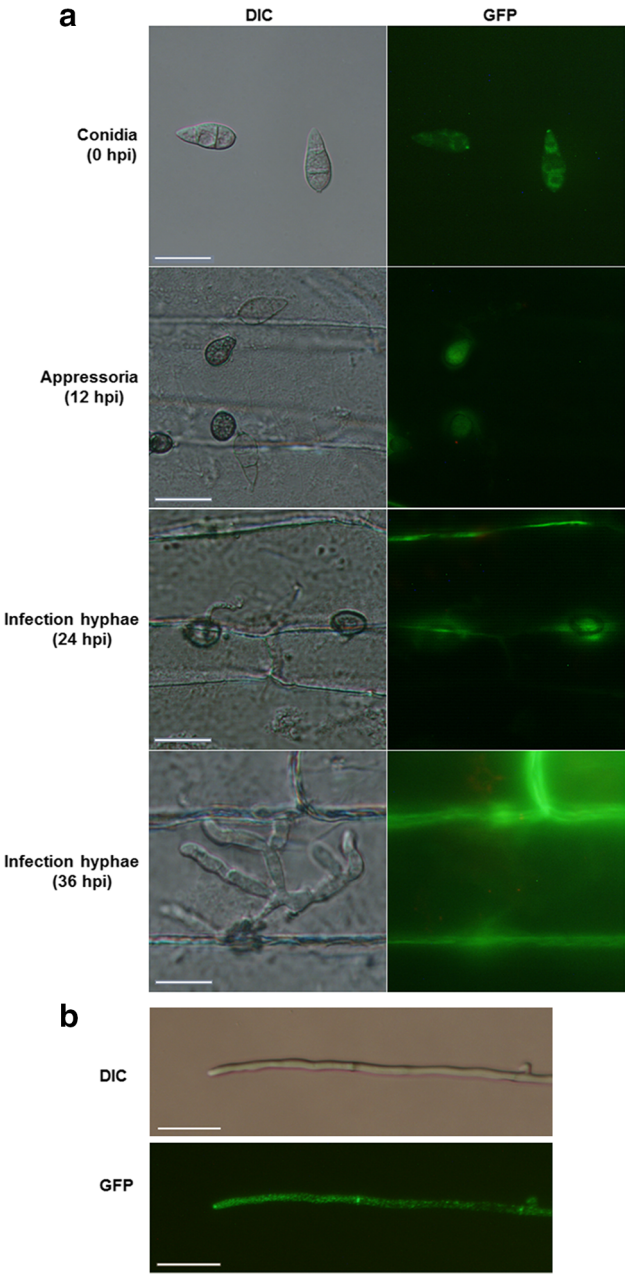

Fig. 5 The expression pattern of *MoSPA2*. **a** Conidia, appressoria (12 hpi), and infection hyphae (24 and 36 hpi) of a complementation transformant of the *ΔMospa2* null mutant MH1 expressing the MoSpa2–eGFP fusion were examined under differential interference contrast (DIC) and epifluorescence (GFP) microscopy. *Bar* 10 μm. **b** Distribution of the MoSpa2-eGFP fusion at the tip of vegetative hyphae. *Bar* 10 μm

MoSPA2 is dispensable for pathogenicity

To investigate the roles of *MoSPA2* on plant infection, conidial suspensions of the *ΔMospa2* null mutant MH1, the complementation transformant CM20, and the wild-type P131 were sprayed on to rice seedlings (Fig. 6a). Plants inoculated with the *ΔMospa2* null mutant MH1 formed numerous typical disease lesions as the complementation transformant CM20 and the wild-type P131 did. Similar results were observed with barley seedlings (Fig. 6b). Moreover, conidia produced by the *ΔMoSpa2* null mutants were normal in appressorium formation and infection hyphae development on barley epidermal cells (Fig. 6c–e). Thus, *MoSPA2* was not required for plant infection.

Discussion

In this study, we identified and functionally characterized *MoSPA2*, a gene encoding a putative spindle pole antigen in *M. oryzae* and plays important roles in vegetative hyphal growth and conidium morphology. By monitoring the subcellular localization of the MoSpa2-GFP fusion in living cells, we could observe an obvious accumulation of the green fluorescence signals located at the tip of vegetative hyphae, which is coincident with its important roles in hyphal growth. Consistently, as a component of the polarisome, Spa2 has been identified from many fungi, including the ascomycete *A. gossypii*, *A. nidulans*, *A. niger*, *N. crassa*, and the basidiomycete *U. maydis*, and all of them were shown to localize at the apex of hyphae and was important to hyphal growth (Carbo and Perez-Martin 2008; Crampin et al. 2005; Knechtle et al. 2003; Meyer et al. 2008; Virag and Harris 2006). We also generated the gene deletion mutants of *FG00932* in *Fusarium graminearum*, which was the ortholog of *SPA2*, and exhibited slow hyphal growth and small colony (data not shown). Therefore, the apex localization of Spa2 is essential to cell polarity and hyphal tip growth. Previously, Spa2 was also found to involve in the direction and control of cell division (Gehrung and Snyder 1990; Roemer et al. 1998). When combined with the observations that no differences were observed in nucleus number of each cell compartment of the vegetative hyphae between the wild-type strain and the *ΔMospa2* null mutant, we speculated that the smaller sizes of the *ΔMospa2* ones should be partially attributed by a shorter cell cycle with the deletion of *MoSPA2*.

Different with the previous findings that most majority of Spa2 was concentrated within the apex of hyphal tips, most of the MoSpa2-GFP fusion in *M. oryzae* was also exhibited dotted distribution among the internal compartment of the sub-apical hyphae and its distribution pattern was acropetal enrichment. This phenomenon might partially explain the reasons on cell polarity growth and smaller size of hyphal cells of the *ΔMospa2* null mutants. Like the emergence of germ tubes from a spore, formation of hyphal branches needs the establishment of a new polarity axis. In some cases, such as *C. albicans*, *A. gossypii*, lateral branching occurs at sites of pre-existing septa (Harris 2008). In other cases, branching sites may be

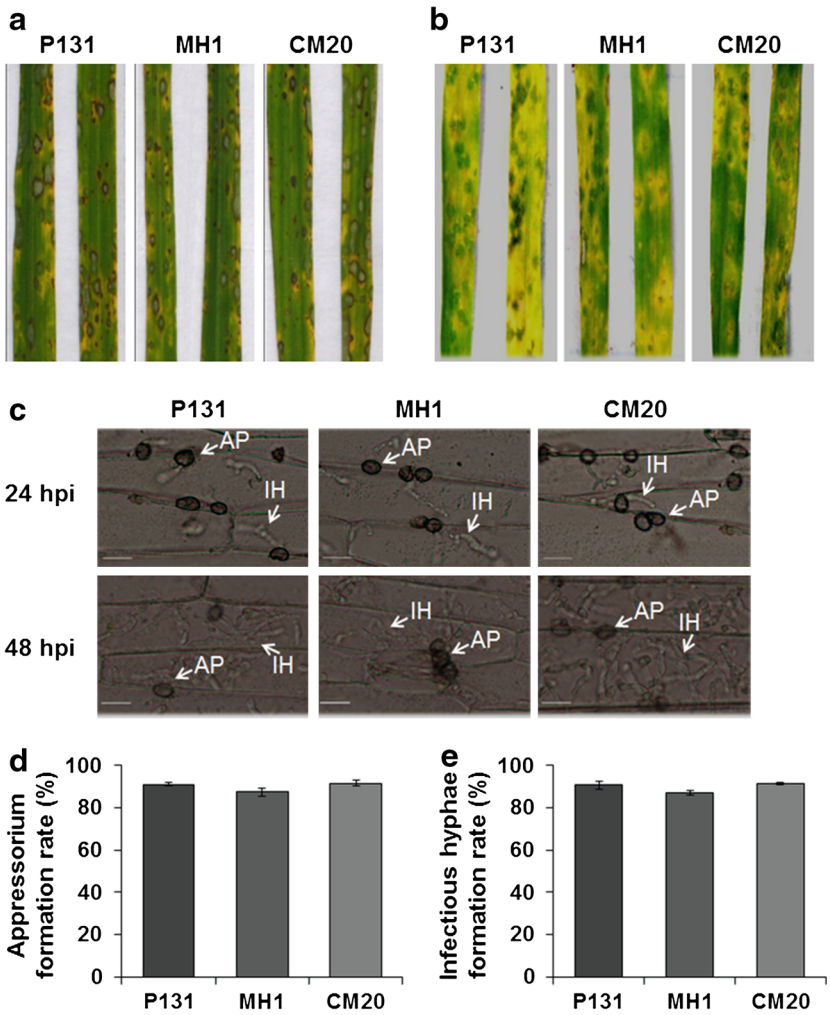

Fig. 6 *MoSPA2* is dispensable for plant infection. Seedlings of rice (**a**) and barley (**b**) were sprayed with conidia of the wild-type P131, the *ΔMospa2* null mutant MH1, and one complementation strain CM20. Disease lesions were examined and photographed at 5–7 dpi. **c** Appressorium formation and infection hyphae developments of P131, MH1, and CM20 on barley epidermal cells at 24 and 48 hpi. *Bar* 20 μm. **d** The appressoria formation rates of P131, MH1, and CM20 at 24 hpi. Means and standard deviations were calculated based on three independent experiments by measuring at least 100 germinated conidia in each replicate. **e** The infection hyphae formation rates of P131, MH1, and CM20 at 48 hpi. Means and standard deviations were calculated based on three independent experiments by measuring at least 100 appressoria in each replicate

selected at random, such as *N. crassa*, and lateral branching generally occurs in the middle hyphal compartment (Harris 2006). *M. oryzae* preferentially forms lateral branching at sites of pre-existing septa, and the MoSpa2–GFP fusions were shown to be septum localized, which might be responsible for more branches of the colony in the strains with the deletion of *MoSPA2*. These observations indicated that MoSpa2 can serve as a marker of polarization and is essential for hyphal branching.

The MoSpa2-GFP fusion was also observed in conidia, and especially a bright green fluorescent spot was observed to localize at the tip of apical or basal cell of conidium where germ tube is produced (Patkar et al. 2010). When combined with the observations that the germination tube usually formed from the cell that had a bright green fluorescent spot of the MoSpa2–GFP fusion, MoSpa2 was supposed to ensure polarity development of conidia despite no obvious differences between the *ΔMospa2* null mutant and the wild type on conidial germination pattern (apical- or basal-cell germination; data not shown). However, cell lengths of the *ΔMospa2* conidia were significantly shorter than the wild-type ones, especially the apical cell, which should be attributed by loss function of *MoSPA2*. During the process of infection-related morphogenesis, no spotted accumulation of the MoSpa2–GFP fusion were observed in appressoria, penetration pegs, and infection hyphae, although weak green fluorescence signals were also rarely detected in them. Consistently, the *ΔMospa2* null mutant had no defects in appressorium formation, penetration peg formation, infection hyphae development, and also virulence toward host plants. Similar results were also found in *U. maydis* (Carbo and Perez-Martin 2008). Therefore, spotted accumulation of the MoSpa2–GFP fusion might reflect the essential functions of *MoSPA2* during the asexual development and conidium morphology, and MoSpa2 has the roles not only in polarity maintenance, but also during early events of polarity establishment. This study also provided solid evidence that there is no direct relevance between vegetative hyphal growth and invasion hyphal development by large scale analysis of pathogenicity genes in the rice blast fungus (Jeon et al. 2007).

Acknowledgments This work was supported by Chinese Universities Scientific Fund (Grant No. 2013XJ012) and National Fundamental Basic Research program (Grant No. 2012CB114002) of the Ministry of Sciences and Technology, China.

Conflict of interest We declared that no conflict of interest exists.

References

Amberg DC, Zahner JE, Mulholland JW, Pringle JR, Botstein D (1997) Aip3p/Bud6p, a yeast actin-interacting protein that is involved in morphogenesis and the selection of bipolar budding sites. Mol Bio Cell 8:729–753

Carbo N, Perez-Martin J (2008) Spa2 is required for morphogenesis but it is dispensable for pathogenicity in the phytopathogenic fungus *Ustilago maydis*. Fungal Genet Biol 45:1315–1327

Crampin H, Finley K, Gerami-Nejad M, Court H, Gale C, Berman J, Sudbery P (2005) *Candida albicans* hyphae have a Spitzenkorper that is distinct from the polarisome found in yeast and pseudohyphae. J Cell Sci 118:2935–2947

Delgehyr N, Lopes CS, Moir CA, Huisman SM, Segal M (2008) Dissecting the involvement of formins in Bud6p-mediated cortical capture of microtubules in *S. cerevisiae*. J Cell Sci 121:3803–3814

Du Y, Shi Y, Yang J, Chen X, Xue M, Zhou W, Peng YL (2013) A serine/threonine-protein phosphatase PP2A catalytic subunit is essential for asexual development and plant infection in *Magnaporthe oryzae*. Curr Genet 59:33–41

Gehrung S, Snyder M (1990) The *SPA2* gene of *Saccharomyces cerevisiae* is important for pheromone-induced morphogenesis and efficient mating. J Cell Biol 111:1451–1464

Gouet P, Courcelle E, Stuart DI, Metoz F (1999) ESPript: analysis of multiple sequence alignments in PostScript. Bioinformatics 15:305–308

Harris SD (2006) Cell polarity in filamentous fungi: shaping the mold. Int Rev Cytol 251:41–77

Harris SD (2008) Branching of fungal hyphae: regulation, mechanisms and comparison with other branching systems. Mycologia 100:823–832

Harris SD (2009) The Spitzenkorper: a signalling hub for the control of fungal development? Mol Microbiol 73:733–736

Jeon J, Park SY, Chi MH, Choi J, Park J, Rho HS, Kim S, Goh J, Yoo S, Choi J, Park JY, Yi M, Yang S, Kwon MJ, Han SS, Kim BR, Khang CH, Park B, Lim SE, Jung K, Kong S, Karunakaran M, Oh HS, Kim H, Kim S, Park J, Kang S, Choi WB, Kang S, Lee YH (2007) Genome-wide functional analysis of pathogenicity genes in the rice blast fungus. Nat Genet 39:561–565

Jones LA, Sudbery PE (2010) Spitzenkorper, exocyst, and polarisome components in *Candida albicans* hyphae show different patterns of localization and have distinct dynamic properties. Eukaryot Cell 9:1455–1465

Knechtle P, Dietrich F, Philippsen P (2003) Maximal polar growth potential depends on the polarisome component AgSpa2 in the filamentous fungus *Ashbya gossypii*. Mol Biol Cell 14:4140–4154

Kohli M, Galati V, Boudier K, Roberson RW, Philippsen P (2008) Growth-speed-correlated localization of exocyst and polarisome components in growth zones of *Ashbya gossypii* hyphal tips. J Cell Sci 121:3878–3889

Lichius A, Yanez-Gutierrez ME, Read ND, Castro-Longoria E (2012) Comparative live-cell imaging analyses of SPA-2, BUD-6 and BNI-1 in *Neurospora crassa* reveal novel features of the filamentous fungal polarisome. PLoS ONE 7:e30372

Lu S, Lyngholm L, Yang G, Bronson C, Yoder OC, Turgeon BG (1994) Tagged mutations at the *Tox1* locus of *Cochliobolus heterostrophus* by restriction enzyme-mediated integration. Proc Natl Acad Sci 91:12649–12653

Meyer V, Arentshorst M, van den Hondel CA, Ram AF (2008) The polarisome component SpaA localises to hyphal tips of *Aspergillus niger* and is important for polar growth. Fungal Genet Biol 45:152–164

Park G, Bruno KS, Staiger CJ, Talbot NJ, Xu JR (2004) Independent genetic mechanisms mediate turgor generation and penetration peg formation during plant infection in the rice blast fungus. Mol Microbiol 53:1695–1707

Patkar RNI, Suresh A, Naqvi NI (2010) MoTea4-mediated polarized growth is essential for proper asexual development and pathogenesis in *Magnaporthe oryzae*. Eukaryot Cell 9:1029–1038

Peng YL, Shishiyama J (1988) Temporal sequence of cytological events in rice leaves infected with *Pyricularia oryzae*. Can J Bot 66:730–735

Roemer T, Vallier L, Sheu YJ, Snyder M (1998) The Spa2-related protein, Sph1p, is important for polarized growth in yeast. J Cell Sci 111(Pt 4):479–494

Saitou N, Nei M (1987) The neighbor-joining method: a new method for reconstructing phylogenetic trees. Mol Biol Evol 4:406–425

Sambrook J, Russell DW (2001) Molecular cloning: a laboratory manual. Cold Spring Harbor Laboratory Press, Cold Spring Harbor

Sheu YJ, Santos B, Fortin N, Costigan C, Snyder M (1998) Spa2p interacts with cell polarity proteins and signaling components involved in yeast cell morphogenesis. Mol Cell Biol 18:4053–4069

Shimizu J, Yoda K, Yamasaki M (1994) The hypo-osmolarity-sensitive phenotype of the *Saccharomyces cerevisiae* hpo2 mutant is due to a mutation in PKC1, which regulates expression of beta-glucanase. Mol Gen Genet 242:641–648

Sweigard JA, Carroll AM, Farrall L, Chumley FG, Valent B (1998) *Magnaporthe grisea* pathogenicity genes obtained through insertional mutagenesis. Mol Plant Microbe Interact 11:404–412

Talbot NJ, Kershaw MJ, Wakley GE, De Vries O, Wessels J, Hamer JE (1996) *MPG1* encodes a fungal hydrophobin involved in surface interactions during infection-related development of *Magnaporthe grisea*. Plant Cell 8:985–999

Tamura K, Dudley J, Nei M, Kumar S (2007) MEGA4: molecular evolutionary genetics analysis (MEGA) software version 4.0. Mol Biol Evol 24:1596–1599

Tcheperegine SE, Gao XD, Bi E (2005) Regulation of cell polarity by interactions of Msb3 and Msb4 with Cdc42 and polarisome components. Mol Cell Biol 25:8567–8580

Valtz N, Herskowitz I (1996) Pea2 protein of yeast is localized to sites of polarized growth and is required for efficient mating and bipolar budding. J Cell Biol 135:725–739

van Drogen F, Peter M (2002) Spa2p functions as a scaffold-like protein to recruit the Mpk1p MAP kinase module to sites of polarized growth. Curr Biol 12:1698–1703

Virag A, Harris SD (2006) Functional characterization of *Aspergillus nidulans* homologues of *Saccharomyces cerevisiae* Spa2 and Bud6. Eukaryot Cell 5:881–895

Xu JR, Hamer JE (1996) MAP kinase and cAMP signaling regulate infection structure formation and pathogenic growth in the rice blast fungus *Magnaporthe grisea*. Genes Dev 10:2696–2706

Yang J, Zhao X, Sun J, Kang Z, Ding S, Xu JR, Peng YL (2010) A novel protein Com1 is required for normal conidium morphology and full virulence in *Magnaporthe oryzae*. Mol Plant Microbe Interact 23:112–123

Zheng XD, Wang YM, Wang Y (2003) *CaSPA2* is important for polarity establishment and maintenance in *Candida albicans*. Mol Microbiol 49:1391–1405